International Journal of Modern Physics: Conference Series
Vol. 1, No. 1 (2010) 1–5
© The Authors
DOI: 10.1142/insert DOI here

Improving neutron/gamma pulse shape discrimination (PSD) of EJ-276 plastic scintillation detectors for nuclear security applications using Monte Carlo simulations

Caroline Holroyd*

School of Engineering, Lancaster University, Lancaster, United Kingdom†
c.holroyd2@lancaster.ac.uk‡

Dr. Michael Aspinall

School of Engineering, Lancaster University, Lancaster, United Kingdom
m.d.aspinall@lancaster.ac.uk

Dr. Tom Deakin

LabLogic Systems Limited, Innovation House, 6 Europa View,
Sheffield, S9 1XH, United Kingdom
tdeakin@lablogic.com

Received (Day Month Year)
Revised (Day Month Year)
Published (Day Month Year)

Plastic scintillators capable of neutron/gamma pulse shape discrimination (PSD) offer a low-cost alternative to organic liquids and crystals for the detection of neutrons in mixed radiation fields for nuclear security applications. Liquid and crystal scintillators have been used for decades for neutron detection, however difficulties with the handling and transportation of such detectors for large-area field applications has motivated a search for solid-state alternatives without a loss of detection capabilities. Plastic scintillators are robust and can easily be manufactured in a variety of shapes and sizes. However, commercially available PSD-capable plastic scintillators have been shown to

.

exhibit generally poorer PSD performance when scaled up to larger sizes. PSD relies on exploiting subtle differences in the shapes of neutron- and gamma-induced pulses, therefore even small variations in the pulse shapes can lead to a noticeable deterioration in the ability of the detector to effectively separate out neutron/gamma pulses. This work reports on the results of Monte Carlo simulation studies conducted to explore the impact of scintillator geometry on the temporal pulse shapes extracted from EJ-276, a PSD-capable plastic scintillator developed by Eljen Technologies. The optical physics capabilities of GEANT4 have been used to simulate the generation and transportation of scintillation photons up to their detection at the photodetector surface. Results show that changes in scintillator size introduce distortion into the pulse shapes, leading to reduced pulse shape discrimination between neutron and gamma pulses. The ability to accurately simulate the temporal pulse shapes from PSD-capable plastic scintillation detectors offers the potential to assess the PSD performance of these detectors prior to fabrication.

Keywords: Neutron detection; plastic scintillators; Monte Carlo simulations.

PACS numbers:

1. Introduction

Radiation Portal Monitors (RPMs) are deployed at international border crossings to detect the illicit trafficking of special nuclear material (SNM). One of the most commonly used neutron detectors in RPMs are ^{3}He gas-filled proportional counters, which exploit the ^{3}He(n,p)^{3}H reaction to detect thermal neutrons[1]. These detectors are non-hazardous, have excellent efficiency for thermal neutron detection, and are insensitive to gamma rays.

However, the probability of neutron capture for ^{3}He decreases with increasing neutron energy. Therefore, these detectors have low efficiency for the detection of fast neutrons. During the thermalization process information about the initial energy of the neutron, its trajectory, and emission time is lost, limiting applications beyond neutron counting[2]. Previously, concerns surrounding potential shortages of ^{3}He has resulted in a search for alternative detectors that meet the requirements for nuclear security applications[3,4].

Fast neutrons can be detected using organic scintillators[4], which exist as crystals, liquids and plastics. The detection mechanism is based on the elastic scattering of neutrons from hydrogen atoms. Scintillation light is emitted when recoiling protons deposit their energy in the scintillator.

Advantages of organics include their hydrogenous composition, fast timing and ability to discriminate between neutron and gamma radiation using the pulse shape analysis technique known as pulse shape discrimination (PSD). PSD enables the separation of neutron and gamma induced pulses based on subtle differences in the shapes of the pulses output from these detectors. PSD exploits the fact that organic scintillators emit light with different time components - known as the fast and slow components - due to the emission of prompt and delayed fluorescence. The fast component is emitted nanoseconds following particle interaction in the scintillator, while the slow component is emitted a few hundred nanoseconds after. Neutrons demonstrate a greater rate of energy loss during interaction than those of gamma-rays. This results in neutrons producing an enhanced proportion of delayed fluorescence compared to gamma-rays[5].

Over the years, various PSD methods have been developed which exploit this property, with the overall aim of achieving the greatest separation between neutron and gamma pulses. One of the most widely used methods is known as the charge comparison method[6]. This method is based on a comparison of the integrals under the pulse, over two different time intervals, typically referred to as the long and short integral. The long integral is the area of the entire pulse while the short integral includes part of the area of the decay tail. The starting point of the short integral is taken from a certain reference point after the peak of the pulse. Since neutron pulses decay more slowly, they have a larger short integral compared to gamma pulses and discrimination is achieved on this basis. The PSD performance of neutron detectors can be quantified by the Figure of Merit (FoM). This is given by FoM = $S/(\delta_{gamma}+\delta_{neutron})$ where S is the separation between neutron and gamma peaks and δ_{gamma} and $\delta_{neutron}$ are the full-width at half maximum (FWHM) of the corresponding peaks. A FoM greater than one generally indicates a good level of PSD.

Organic single crystals have been used successfully for decades for neutron detection due to their excellent scintillator light output (LO) and PSD performance. However, single crystals such as stilbene are expensive and there are difficulties associated with the transportation of large-area detectors[7]. Liquid scintillators can be constructed in large volumes, however there are problems with handling and field applications due to fears surrounding potential leaks. These difficulties have motivated a search for alternative, solid-state scintillators for large-area field applications that can replace liquids and crystals without a loss of detection capability.

PSD-capable plastic scintillators offer a promising, solid-state alternative to the use of organic liquids and crystals for neutron detection. They are inexpensive, robust, easy to transport and can be fabricated in a variety of shapes and sizes. Early studies to develop efficient PSD in plastics resulted in unstable materials[8]. This subsequently led to assumptions surrounding the inherently poor PSD in plastics[9]. However, in 2012 the first plastic scintillators with efficient PSD were developed at Lawrence Livermore National Laboratory in the United States[10]. The LO and PSD of these small-scale plastics (25 mm x 25 mm cylinders) were found to compare favorably with liquid scintillators of the same size. However, when the first commercial PSD-capable plastics became available at larger sizes through Eljen Technologies under the trade name EJ-299, studies reported generally poorer PSD performance of plastics compared to liquids and crystals[11–13]. In 2018, EJ-299-33 was replaced by EJ-276. These new plastics offered improved radiation hardness and long-term stability[14]. Comparison studies showed improved PSD performance of EJ-276 compared to EJ-299-33; however, organic liquids and crystals still demonstrated superior PSD[15].

Deterioration in PSD performance has been observed due to changes in scintillator shape and volume. The PSD performance of cube and right-cylindrical geometries of EJ-309 liquid scintillators has been shown to decrease with increasing volume of scintillator, with the deterioration worsening at higher energies[16]. The effect of scintillator geometry on the PSD performance of the plastic scintillator EJ-299-33 was investigated for two geometries between (15x15x15) mm and (125 x 125 x 125) mm[17]. Results showed a decrease in FoM values as the scintillator geometry moved from a cube-like shape to a flatpanel shape. At an energy threshold of 1 MeVee the FoM for a (120x25x15) mm sample was found to be 20% worse than that obtained for the (25x25x15) mm sample.

This paper reports on the results of Monte Carlo simulation studies conducted to investigate how the size and shape of the scintillator impacts on the temporal pulse shapes output from an EJ-276 plastic scintillation detector for two different geometries, as the size is increased. EJ-276 has been suggested as a possible alternative to liquid scintillators for homeland security applications[18]. The aim of this study is to understand the reasons behind the poorer PSD performance observed for large-area PSD plastics through analysis of the n/γ pulse shapes. Since PSD relies on exploiting subtle differences in the shapes of neutron and gamma induced pulses, even small variations in the output pulse shapes can lead to a noticeable deterioration in the ability of the detector to separate out signals due to the different radiation types.

The Monte Carlo toolkit GEANT4 has been shown to be capable of correctly simulating the timing properties of individual scintillation photons for organic[11,19–21] and inorganic[22] scintillation detectors. Simulations enable the decoupling of other factors observed to impact on the PSD performance of scintillation detectors, such as the photodetector response and data acquisition electronics[23,24]. Also, it can be difficult to make comparisons between the PSD performance of detectors experimentally due to differences in detector type, photodetector, read-out electronics and the PSD method used.

2. Methodology

GEANT4 is an object-oriented Monte Carlo toolkit developed by CERN for simulating the passage of particles through matter[25]. An EJ-276 plastic scintillator has been built using GEANT4 version 10.7 with input parameters obtained from the EJ-276 data sheet, provided by Eljen Technologies[26]. A cube and a slab geometry have been constructed. These are shown in Figures 1 and 2, respectively, where the location of the photodetector is highlighted in red. Experimental values for the scintillator decay times and their relative intensities for neutron and gamma radiation have been used[13] to improve the accuracy of the simulations. For each run, 10^4 primary particles of gamma-rays and neutrons were simulated using an isotropic point source which generated approximately 10^7 scintillation photons for each geometry. An energy of 2 MeV was chosen for all primary particles to ensure the number of particles generated remained constant for the two radiation types. The source was placed at the centre of the detector to ensure pulse shape features would be the result of light transport through the detector volume.

The physics list used for all simulations described in this paper is the reference physics list QGSP_BIC_HP_EMZ. G4OpticalPhysics has been included for the generation and transportation of scintillation photons[25].

Individual scintillation photons have been tracked up to their detection at the surface of a photodetector with a bialkali photocathode, which is registered as a G4SensitiveDetector. The simulated pulses represent the arrival time distribution of scintillation photons at the surface of the photodetector. Data was plotted and analysed using MATLAB.

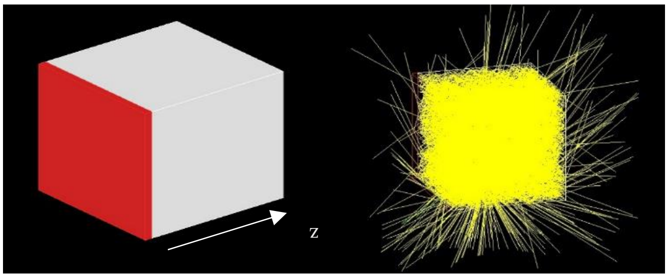

Figure 1. GEANT4 simulated cube geometry before (left) and after (right) scintillation.

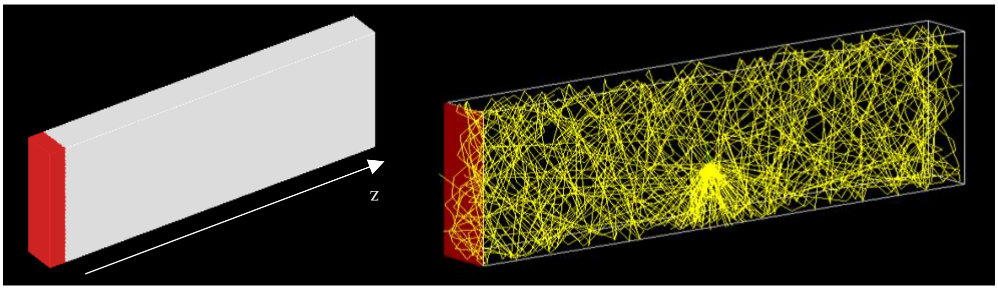

Figure 2. GEANT4 simulated slab geometry before (left) and after (right) scintillation.

3. Results

3.1. Cube geometry

In Figures 3 and 4, the time-dependent scintillation light pulses due to gamma-ray interactions in the EJ-276 scintillator for a cube geometry of varying size, from 10 mm to 100 mm, are shown. When the scintillator size is small (< 100 mm), the shapes of the pulses approximate that of a Gaussian distribution. As the size of the scintillator is increased, the width of the pulse also increases due to scintillation photons needing to travel further in the scintillator volume before being detected at the surface of the photocathode. As the scintillator size approaches 100 mm, distortions begin to appear in the peak of the pulse.

Beyond 100 mm, the rising edge becomes steeper and further distortion appears in the decay tail of the pulse, the crucial feature for PSD. In Figures 5 and 6, ‘humps’ appear in the pulses, beginning at the peak of the pulse and then travelling down the pulse tail as the scintillator increases past 500 mm in all dimensions. The width of the pulses shorten and lose their Gaussian shape.

For neutron pulses, shown in Figures 7, 8, 9 and 10, the pulse shape distortions appear when the cube scintillator size is increased to 200 mm in all dimensions.

Figures 11 and 12 show the neutron/gamma pulses plotted together for the smallest (10 mm) and largest (1000 mm) size of cube scintillator, respectively. Separation between the pulses can be observed in the decay tail of the pulses for the 10 mm cube, shown in Figure 11. Separation between the pulses can also be observed in Figure 12 for the 1000 mm cube, however the introduction of distortions into the pulse shapes means a clear separation is not observed until approximately 35 ns and there is a greater overlap between pulses compared with Figure 11.

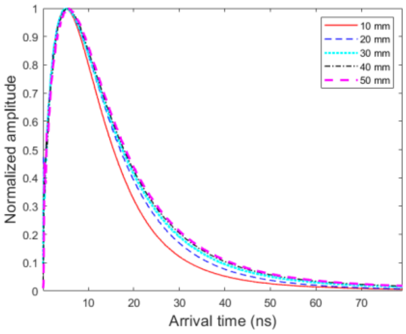

Figure 3. Simulated gamma pulse shapes for varying sizes of EJ-276 cubic scintillator, from 10 mm to 50 mm.

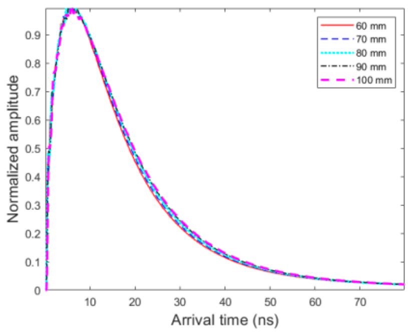

Figure 4. Simulated gamma pulse shapes for varying sizes of EJ-276 cubic scintillator, from 60 mm to 100 mm.

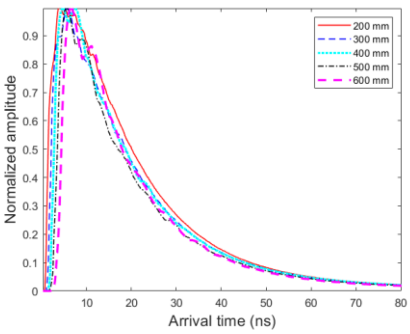

Figure 5. Simulated gamma pulse shapes for varying sizes of EJ-276 cubic scintillator, from 200 mm to 600 mm.

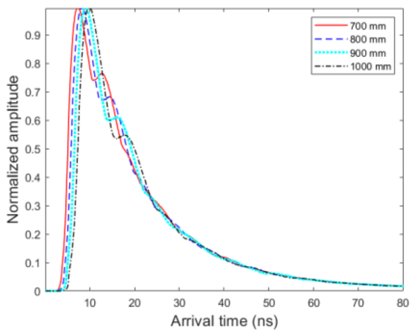

Figure 6. Simulated gamma pulse shapes for varying sizes of EJ-276 cubic scintillator, from 700 mm to 1000 mm.

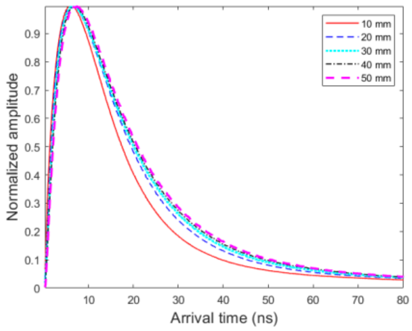

Figure 7. Simulated neutron pulse shapes for varying sizes of EJ-276 cubic scintillator, from 10 mm to 50 mm.

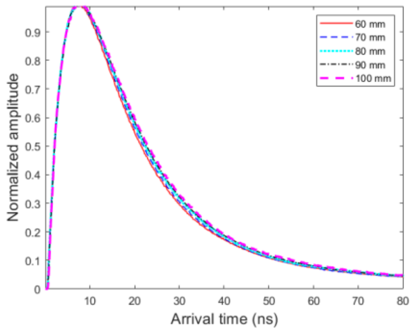

Figure 8. Simulated neutron pulse shapes for varying sizes of EJ-276 cubic scintillator, from 60 mm to 100 mm.

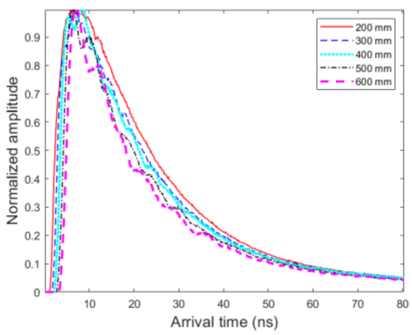

Figure 9. Simulated neutron pulse shapes for varying sizes of EJ-276 cubic scintillator, from 200 mm to 600 mm.

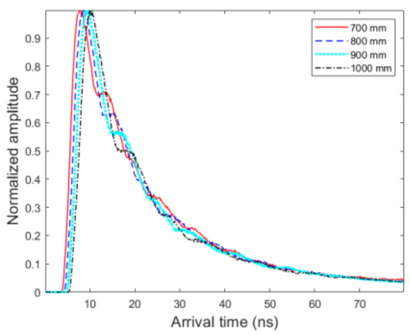

Figure 10. Simulated neutron pulse shapes for varying sizes of EJ-276 cubic scintillator, from 700 mm to 1000 mm.

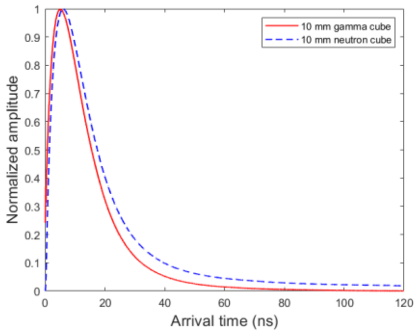

Figure 11. Simulated neutron (blue, dotted line) and gamma (red, solid line) pulse shapes for 10 mm cube scintillator.

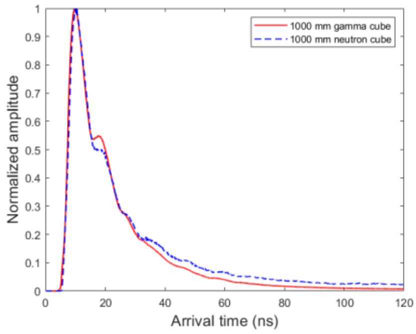

Figure 12. Simulated neutron (blue, dotted line) and gamma (red, solid line) pulse shapes for 1000 mm cube scintillator.

3.2. Slab geometry

The simulated time-dependent scintillation light pulses due to gamma-ray interactions in the EJ-276 scintillator for a slab geometry of varying size, from 60 mm to 1000 mm, are shown in Figures 13, 14 and 15. For the slab geometry, shown in Figure 2, the scintillator is increased in the Z-direction while the X and Y direction remains constant with values of 10 mm and 25 mm, respectively. Distortion begins to appear in the pulses as the size of the slab is increased to 200 mm in the Z-direction and further distortion appears in the form of ‘humps’ as the slab size is increased up to 1000 mm.

The simulated time-dependent scintillation light pulses due to neutron interactions in the slab scintillator are shown in Figures 16, 17 and 18 and show the same evidence of distortion to the pulse shapes, which increases as the size of the slab approaches 1000 mm in the Z-direction.

Figures 19 and 20 show the neutron/gamma pulses plotted together for the smallest (60 mm) and largest (1000 mm) size of slab scintillator, respectively. Separation between the pulses can be observed for both scintillator sizes despite the pulse shape distortions evident in the neutron/gamma pulses for the 1000 mm slab scintillator.

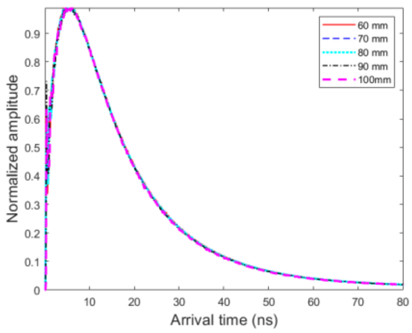

Figure 13. Simulated gamma pulse shapes for varying sizes of EJ-276 slab scintillator, from 60 mm to 100 mm.

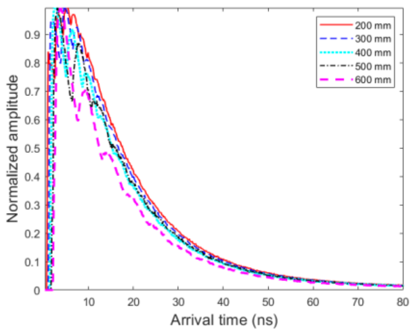

Figure 14. Simulated gamma pulse shapes for varying sizes of EJ-276 slab scintillator, from 200 mm to 600 mm.

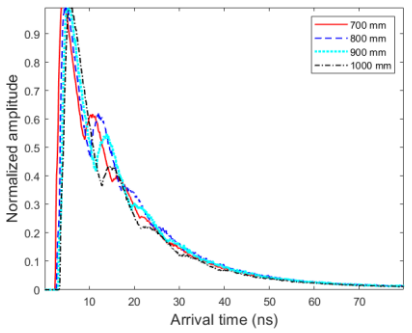

Figure 15. Simulated gamma pulse shapes for varying sizes of EJ-276 slab scintillator, from 700 mm to 1000 mm.

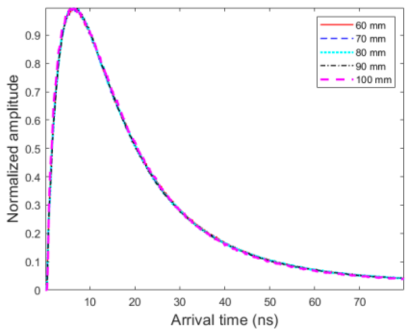

Figure 16. Simulated neutron pulse shapes for varying sizes of EJ-276 slab scintillator, from 60 mm to 100 mm.

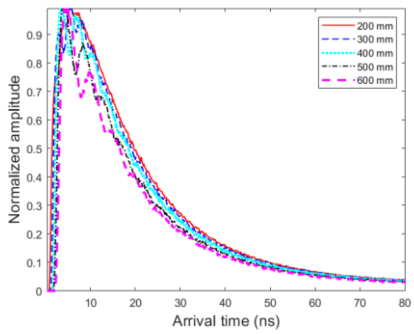

Figure 17. Simulated neutron pulse shapes for varying sizes of EJ-276 slab scintillator, from 200 mm to 600 mm.

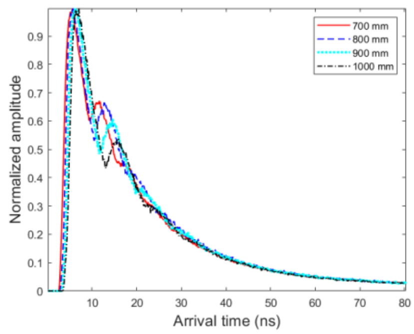

Figure 18. Simulated neutron pulse shapes for varying sizes of EJ-276 slab scintillator, from 700 mm to 1000 mm.

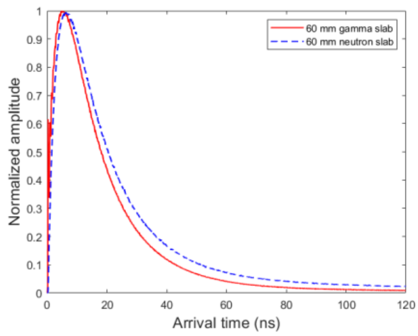

Figure 19. Simulated neutron (blue, dotted line) and gamma (red, solid line) pulse shapes for 60 mm slab scintillator.

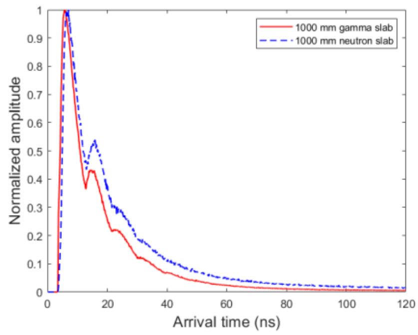

Figure 20. Simulated neutron (blue, dotted line) and gamma (red, solid line) pulse shapes for 1000 mm slab scintillator.

4. Conclusions and future work

In this work, the Monte Carlo toolkit GEANT4 has been used to simulate the time-dependent neutron/gamma pulses from EJ-276, a PSD-capable plastic scintillator. Simulations show that as the size of the scintillator is increased for two different geometries, artifacts appear which distort the shapes of the pulses and results in them losing their Gaussian appearance.

The appearance of 'humps' in the neutron/gamma pulse shapes may be the result of increased variation in the travel time of scintillation photons arriving at the surface of the photocathode, as the size of the scintillator is increased. Scintillation photons travelling in the opposite direction to the photocathode have to travel a longer distance and may be reflected multiple times before being detected; conversely, those travelling in the direction of the photocathode are detected almost instantaneously and contribute to the initial peak of the pulse.

Although distortions are observed for both the slab and cube geometry, the separation between neutron and gamma pulses is greater for the largest slab geometry than for the largest cube geometry. This is likely due to the larger scintillator volume of the cube, resulting in a greater variation in photon travel times.

These distortions may contribute to the observed poorer PSD performance of plastic scintillators when they are scaled up to larger sizes, however further analysis is required to quantify the impact of these distortions on the overall PSD performance of large-area PSD plastics.

Future work will involve generating a large number of simulated n/γ pulses in order to perform PSD for the two geometries. The accuracy of the simulations developed is limited by not including the response of the photodetector and read-out electronics, factors known to influence the shapes of the pulses. Therefore, in order to improve the accuracy of the simulations and enable a comparison with experimental measurements, future work will involve including the photodetector response and quantifying its impact on the shapes of the simulated pulses.

Acknowledgements

This work was funded by Lancaster University, UK, and the Engineering and Physical Sciences Research Council (EPSRC).

References

[1] A. Tomanin, P. Peerani, and G. Janssens-Maenhout, "On the optimisation of the use of 3He in radiation portal monitors," Nucl. Instruments Methods Phys. Res. Sect. A Accel. Spectrometers, Detect. Assoc. Equip. **700**, 81–85 (2013).

[2] D.C. Stromswold, A.J. Peurrung, R.R. Hansen, and P.L. Reeder, "Direct Fast-Neutron Detection," Prep. U.S. Dep. Energy under Contract DE-AC06-76RL0 1830 Pacific, (1998).

[3] R.T. Kouzes, J.H. Ely, L.E. Erikson, W.J. Kernan, A.T. Lintereur, E.R. Siciliano, D.L. Stephens,

D.C. Stromswold, R.M. Van Ginhoven, and M.L. Woodring, "Neutron detection alternatives to 3He for national security applications," Nucl. Instruments Methods Phys. Res. Sect. A Accel. Spectrometers, Detect. Assoc. Equip. **623**(3), 1035–1045 (2010).

[4] R.T. Kouzes, A.T. Lintereur, and E.R. Siciliano, "Progress in alternative neutron detection to address the helium-3 shortage," Nucl. Instruments Methods Phys. Res. Sect. A Accel. Spectrometers, Detect. Assoc. Equip. **784**, 172–175 (2015).

[5] J.B. Birks, *The Theory and Practice of Scintillation Counting* (Pergamon Press, London, 1964).

[6] F.D. Brooks, "A scintillation counter with neutron and gamma-ray discriminators," Nucl. Instruments Methods **4**(3), 151–163 (1959).

[7] T.A. Laplace, B.L. Goldblum, J.E. Bevins, D.L. Bleuel, E. Bourret, J.A. Brown, E.J. Callaghan, J.S. Carlson, P.L. Feng, G. Gabella, K.P. Harrig, J.J. Manfredi, C. Moore, F. Moretti, M. Shinner, A. Sweet, and Z.W. Sweger, "Comparative scintillation performance of EJ-309, EJ-276, and a novel organic glass," J. Instrum. **15**(11), P11020–P11020 (2020).

[8] P.G.A.S. Scintillators, "Pulse Shape Discrimination in - ' PU ' V-," **4**, 35–38 (1959).

[9] F.D. Brooks, "Development of organic scintillators," Nucl. Instruments Methods **162**(1–3), 477–505 (1979).

[10] N. Zaitseva, B.L. Rupert, I. PaweŁczak, A. Glenn, H.P. Martinez, L. Carman, M. Faust, N. Cherepy, and S. Payne, "Plastic scintillators with efficient neutron/gamma pulse shape discrimination," Nucl. Instruments Methods Phys. Res. Sect. A Accel. Spectrometers, Detect. Assoc. Equip. **668**, 88–93 (2012).

[11] C. Liao, and H. Yang, "N/γ Pulse shape discrimination comparison of EJ301 and EJ339A liquid scintillation detectors," Ann. Nucl. Energy **69**, 57–61 (2014).

[12] S.A. Pozzi, M.M. Bourne, and S.D. Clarke, "Pulse shape discrimination in the plastic scintillator EJ-299-33," Nucl. Instruments Methods Phys. Res. Sect. A Accel. Spectrometers, Detect. Assoc. Equip. **723**, 19–23 (2013).

[13] J. Iwanowska-Hanke, M. Moszynski, L. Swiderski, P. Sibczynski, T. Szczesniak, T. Krakowski, and P. Schotanus, "Comparative study of large samples (2)," J. Instrum. **9**(6), (2014).

[14] N.P. Zaitseva, A.M. Glenn, A.N. Mabe, M.L. Carman, C.R. Hurlbut, J.W. Inman, and S.A. Payne, "Recent developments in plastic scintillators with pulse shape discrimination," Nucl. Instruments Methods Phys. Res. Sect. A Accel. Spectrometers, Detect. Assoc. Equip. **889**(February), 97–104 (2018).

[15] M. Grodzicka-Kobylka, T. Szczesniak, M. Moszyński, K. Brylew, L. Swiderski, J.J. Valiente-Dobón, P. Schotanus, K. Grodzicki, and H. Trzaskowska, "Fast neutron and gamma ray pulse shape discrimination in EJ-276 and EJ-276G plastic scintillators," J. Instrum. **15**(3), (2020).

[16] M. Ellis, C. Tintori, P. Schotanus, K. Duroe, P.A. Kendall, and G. Mini, in *IEEE Nucl. Sci. Symp. Conf. Rec.* (IEEE, 2013), pp. 1–6.

[17] C. Payne, P.J. Sellin, M. Ellis, K. Duroe, A. Jones, M. Joyce, G. Randall, and R. Speller, "Neutron/gamma pulse shape discrimination in EJ-299-34 at high flux," 2015 IEEE Nucl. Sci. Symp. Med. Imaging Conf. NSS/MIC 2015, 1–5 (2016).

[18] M.E. Ellis, K. Duroe, and P.A. Kendall, "Pulse-shape discrimination scintillators for homeland security applications," Int. J. Mod. Phys. Conf. Ser. **44**(2010), 1660214 (2016).

[19] S. Riggi, P. La Rocca, E. Leonora, D. Lo Presti, G.S. Pappalardo, F. Riggi, and G. V. Russo, "Geant4 simulation of plastic scintillator strips with embedded optical fibers for a prototype of tomographic system," Nucl. Instruments Methods Phys. Res. Sect. A Accel. Spectrometers, Detect. Assoc. Equip. **624**(3), 583–590 (2010).

[20] Z.S. Hartwig, and P. Gumplinger, "Simulating response functions and pulse shape discrimination

for organic scintillation detectors with Geant4," Nucl. Instruments Methods Phys. Res. Sect. A Accel. Spectrometers, Detect. Assoc. Equip. **737**, 155–162 (2014).
[21] H. Xing, X. Yu, J. Zhu, L. Wang, J. Ma, S. Liu, L. Li, L. Chen, C. Tang, and Q. Yue, "Simulation study of the neutron-gamma discrimination capability of a liquid scintillator neutron detector," Nucl. Instruments Methods Phys. Res. Sect. A Accel. Spectrometers, Detect. Assoc. Equip. **768**, 1–8 (2014).
[22] R. Ogawara, and M. Ishikawa, "Signal pulse emulation for scintillation detectors using Geant4 Monte Carlo with light tracking simulation," Rev. Sci. Instrum. **87**(7), (2016).
[23] M. Flaska, M. Faisal, D.D. Wentzloff, and S.A. Pozzi, "Influence of sampling properties of fast-waveform digitizers on neutron-gamma-ray, pulse-shape discrimination for organic scintillation detectors," Nucl. Instruments Methods Phys. Res. Sect. A Accel. Spectrometers, Detect. Assoc. Equip. **729**, 456–462 (2013).
[24] C. Hellesen, M. Skiba, G. Ericsson, E. Andersson Sundén, F. Binda, S. Conroy, J. Eriksson, and M. Weiszflog, "Impact of digitization for timing and pulse shape analysis of scintillator detector signals," Nucl. Instruments Methods Phys. Res. Sect. A Accel. Spectrometers, Detect. Assoc. Equip. **720**, 135–140 (2013).
[25] J. Allison, K. Amako, J. Apostolakis, H. Araujo, P.A. Dubois, M. Asai, G. Barrand, R. Capra, S. Chauvie, R. Chytracek, G.A.P. Cirrone, G. Cooperman, G. Cosmo, G. Cuttone, G.G. Daquino, M. Donszelmann, M. Dressel, G. Folger, F. Foppiano, J. Generowicz, V. Grichine, S. Guatelli, P. Gumplinger, A. Heikkinen, I. Hrivnacova, A. Howard, S. Incerti, V. Ivanchenko, T. Johnson, F. Jones, T. Koi, R. Kokoulin, M. Kossov, H. Kurashige, V. Lara, S. Larsson, F. Lei, F. Longo, M. Maire, A. Mantero, B. Mascialino, I. McLaren, P.M. Lorenzo, K. Minamimoto, K. Murakami, P. Nieminen, L. Pandola, S. Parlati, L. Peralta, J. Perl, A. Pfeiffer, M.G. Pia, A. Ribon, P. Rodrigues, G. Russo, S. Sadilov, G. Santin, T. Sasaki, D. Smith, N. Starkov, S. Tanaka, E. Tcherniaev, B. Tomé, A. Trindade, P. Truscott, L. Urban, M. Verderi, A. Walkden, J.P. Wellisch, D.C. Williams, D. Wright, H. Yoshida, and M. Peirgentili, "Geant4 developments and applications," IEEE Trans. Nucl. Sci. **53**(1), 270–278 (2006).
[26] Eljen Technologies, "Ej-276D," (888), 79556 (2023).